

Clumpiness enhancement of charged cosmic rays from dark matter annihilation with Sommerfeld effect

Qiang Yuan¹, Xiao-Jun Bi^{2,1}, Jia Liu³, Peng-Fei Yin³, Juan Zhang¹ and Shou-Hua Zhu³

¹ *Key Laboratory of Particle Astrophysics, Institute of High Energy Physics,
Chinese Academy of Sciences, Beijing 100049, P. R. China*

² *Center for High Energy Physics, Peking University, Beijing 100871, P.R. China*

³ *Institute of Theoretical Physics & State Key Laboratory of Nuclear Physics and Technology,
Peking University, Beijing 100871, P.R. China*

(Dated: October 30, 2018)

Boost factors of dark matter annihilation into antiprotons and electrons/positrons due to the clumpiness of dark matter distribution are studied in detail in this work, taking the Sommerfeld effect into account. It has been thought that the Sommerfeld effect, if exists, will be more remarkable in substructures because they are colder than the host halo, and may result in a larger boost factor. We give a full calculation of the boost factors based on the recent N-body simulations. Three typical cases of Sommerfeld effects, the non-resonant, moderately resonant and strongly resonant cases are considered. We find that for the non-resonant and moderately resonant cases the enhancement effects of substructures due to the Sommerfeld effect are very small ($\sim \mathcal{O}(1)$) because of the saturation behavior of the Sommerfeld effect. For the strongly resonant case the boost factor is typically smaller than $\sim \mathcal{O}(10)$. However, it is possible in some very extreme cases that DM distribution is adopted to give the maximal annihilation the boost factor can reach up to ~ 1000 . The variances of the boost factors due to different realizations of substructures distribution are also discussed in the work.

PACS numbers: 95.35.+d, 95.85.Ry, 96.50.S-

I. INTRODUCTION

The recent observations of the positron excess by PAMELA [1] and the electron excess by ATIC [2] and PPB-BETS [3] have stimulated extensive discussions. The proposed expla-

nations include both the classical astrophysical processes (e.g., [4]) and possible new physics like dark matter (DM) annihilation or decay (e.g. [5]). For the annihilating DM scenario a “boost factor” of order 1000 of the annihilation rate, compared to that to produce the correct relic DM density thermally at the early Universe, is needed to produce enough electrons and positrons to fit the data. Although the newly published Fermi result on the electron spectrum [6] does not reproduce the ATIC sharp “bump” at 300 – 800 GeV, however, to explain the excess at Fermi by DM annihilation requires a similar boost factor [7].

There are several mechanisms suggested to generate the boost factor, including the DM substructures or DM mini-spikes [8, 9, 10], nonthermal production of DM [11], the Sommerfeld effect (SE, [12, 13, 14, 15, 16]) and the Breit-Wigner resonance enhancement [17]. The boost factor due to DM substructures is a natural expectation as N-body simulation shows that there are a large amount of substructures exist in the Milky Way (MW) halo [18]. However, the detailed calculation based on the N-body simulation shows that the boost factor from DM substructures is generally less than ~ 10 ([19], hereafter we refer it as Paper I). Although a single DM clump which is close enough to the Earth may be possible to give large boost factor, it is found such a case has very small probability to survive in a realistic DM distribution model [10, 20]. Therefore, additional boost effect like the SE or Breit-Wigner resonance effect is still necessary in a DM picture to account for the observational data.

Therefore it is necessary to extend the previous discussions of Paper I on the boost factor due to DM clumps to take into account the SE. Furthermore, such a study is also very important for the indirect searches of DM. The SE or Breit-Wigner enhancement is generally related with the velocity dispersion of DM particles. Comparing with the MW halo, the DM in smaller structures is colder and can give larger annihilation signals [21, 22]. In addition, if the DM substructures can contribute a proper fraction to the locally observed electrons/positrons, the boost factor of the Galactic center (GC) can be suppressed due to the tidal destroy of substructures in the inner Galaxy, and can avoid the strong constraints from γ -ray and radio emission [23, 24, 25, 26].

In Refs. [21, 22] the SE in dwarf galaxies and DM subhaloes has been investigated. However, in their works only the effect on the source luminosity is considered. The propagation of the charged particles, especially the most relevant electrons/positrons, is not included. In this work, we will study the boost factor of DM substructures on the electron/positrons and antiprotons after incorporating the SE.

To be clear, in the following part of this paper we will refer to the enhancement effect of DM substructures with respect to the smooth component as the “boost factor” (see definition in Sec. V). For the SE induced enhancement of the smooth component compared with the thermal production cross section we will directly call it as “SE enhancement”.

The paper is organized as follows. We first describe the SE in the next section. Then we discuss the configurations of the DM substructures in Sec. III. The propagation models and definition of boost factors are simply addressed in Sec. IV. In Sec. V we discuss the results of the boost factors from DM substructures including SE. Finally we give the summary and conclusion.

II. THE SOMMERFELD EFFECT

In the calculation of the DM annihilation cross section at low kinetic energy regime, some non-perturbative effects may arise due to new “long-range” interaction. It is called “Sommerfeld effect” which requires to sum all ladder diagrams due to the exchange of some light scalars or gauge bosons between two incoming DM particles. This effect could lead to significant enhancement of the annihilation cross section at small relative velocity. To a good approximation, one can simply multiply a factor S to the tree-level annihilation cross section. In the calculation of such factor, we use the simplified quantum mechanical method in literatures by solving the radial Schrödinger equation with a Yukawa potential $V(r) = -\frac{\alpha}{r}e^{-m_\phi r}$ [13, 14]

$$\frac{1}{m_\chi}\psi''(r) + \frac{\alpha}{r}e^{-m_\phi r}\psi(r) = -m_\chi\beta^2\psi(r), \quad (1)$$

where $\psi(r)$ is the reduced two-body wave function, m_χ and m_ϕ are the masses of DM and the new mediating boson respectively, β is the velocity of DM in the center-of-mass frame. In this work, we only consider the simplest situation in which the new mediator is a light scalar or Abelian gauge boson. In addition, we only take into account the incoming DM particles with S wave (calculation for arbitrary l th partial wave could be found in Refs. [27, 28]).

As described in Ref. [14], there are two equivalent methods to achieve S : (1) solving the Schrödinger equation with outgoing boundary condition $\psi'(r)/\psi(r) \rightarrow im_\chi\beta$ as $r \rightarrow \infty$, then S is given by $S = |\psi(\infty)|^2/|\psi(0)|^2$; (2) using boundary condition $\psi(r)/r \rightarrow \text{constant}$

as $r \rightarrow 0$, S is given by $S = |\psi'(0)/k|^2$, where k is the momentum defined as $k = m_\chi \beta$. Generally Eq.(1) needs to be solved numerically.

In this work, we follow the method of Ref. [27] to get S numerically. We substitute $x = kr$ and $\phi(x) = C\psi(r)/kr$ into Eq. (1) (C is a constant), then solve it with boundary condition as $\phi(0) = 1$. We can normalize the solution at infinity as $F(x) \equiv x\phi(x) \rightarrow C \cdot \sin(x + \delta)$, and we have $C^2 = F^2(x) + F^2(x + \pi/2)$ when x is large enough. Using the formula $S = |\psi'(0)/k|^2$, the SE enhancement factor is obtained as $1/C^2$.

To achieve a more realistic result, we also need to take into account the speed distribution of DM particles [22, 29]. After simply choosing Maxwell-Boltzmann distribution as an acceptable approximation, the averaged SE enhancement is given by

$$\bar{S} = \frac{x}{K_2(x)} \int_0^\infty dp' p'^2 \exp\left(-x\sqrt{1+p'^2}\right) S(\beta), \quad (2)$$

where x is defined as $x = m_\chi/T$, $K_2(x)$ denotes the second order modified Bessel function of the second type, $p' = \beta/\sqrt{1-\beta^2}$ is the normalized DM momentum. When the DM particles are non-relativistic in the MW, Eq.(2) can be written as

$$\bar{S} = \sqrt{\frac{2}{\pi}} \frac{1}{\sigma^3} \int_0^{v_{esc}} dv v^2 \exp\left(-\frac{v^2}{2\sigma^2}\right) S(v), \quad (3)$$

where v and σ are the velocity and velocity dispersion of DM respectively, v_{esc} is the escape velocity in the MW. It is obvious that if the behavior of S are $S \sim 1/v$ and $S \sim 1/v^2$, the average SE enhancement will have similar form $\bar{S} \sim 1/\sigma$ and $\bar{S} \sim 1/\sigma^2$ respectively [22].

Some illustrations of the SE enhancements are shown in Fig. 1. In the upper two panels the variations of the pre-averaged enhancement factor S with model parameters are shown. The results are similar with that given in Refs. [21, 22]. From the top-right panel we can see that there are resonant structures, especially for small velocity β . If the parameters are tuned to approach the resonant region, very large boost factors can be achieved. In the bottom-left panel, we show the average SE enhancement factor \bar{S} as a function of the velocity dispersion, for several values of m_ϕ : close to or away from the resonance peak. In this calculation, we fix the mass of DM particle as $m_\chi = 1$ TeV, and the coupling constant in the Yukawa potential as $\alpha = 1/30$. Two series of parameter m_ϕ , around the two peaks ~ 20 GeV and ~ 1.3 GeV, are shown in this panel. We can clearly see the ‘‘temperature’’ dependence of the SE from this figure. It is shown that at the early stage of the evolution of the universe, when the DM is hot, the SE enhancement is negligible. When DM particles cool down, \bar{S} become

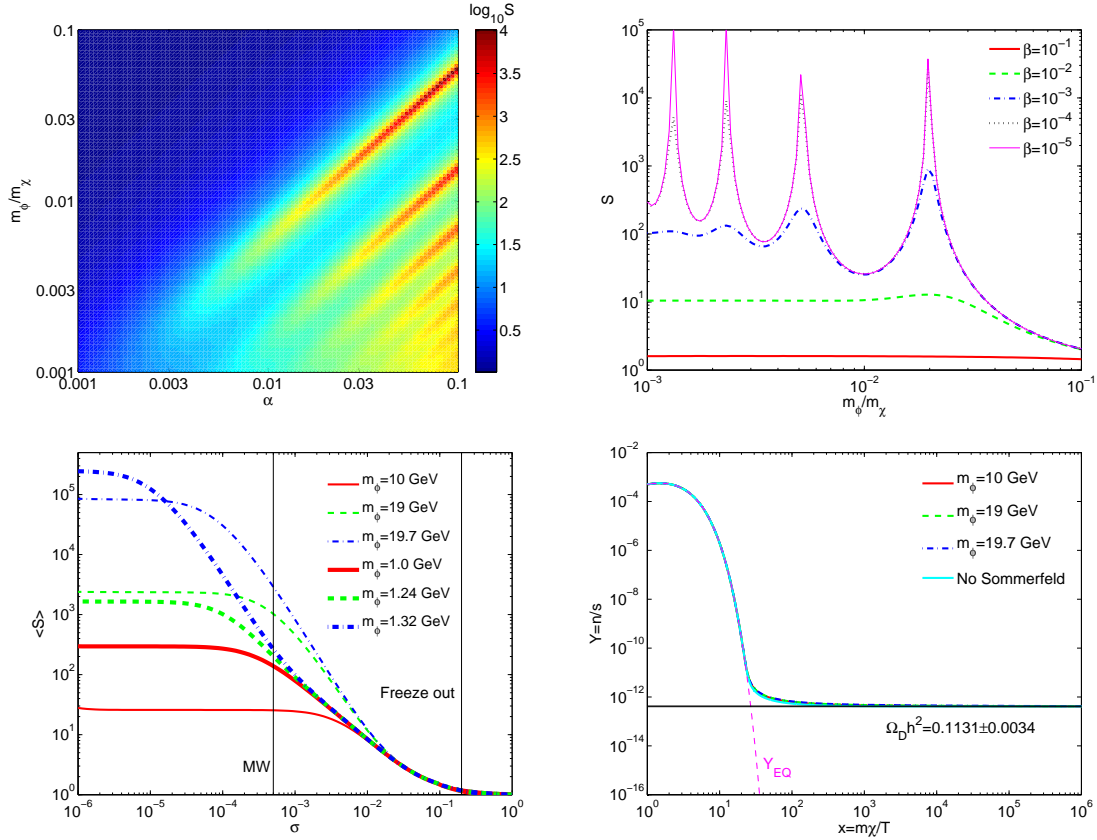


FIG. 1: Top-left: the SE enhancement factor S as a function of coupling constant α and m_ϕ/m_χ , for a single velocity $\beta = 220 \text{ km s}^{-1}$; top-right: S as a function of m_ϕ/m_χ for several velocity β , in which α is fixed to be $1/30$; bottom-left: the average SE enhancement factor vs. velocity dispersion (in unit of light speed) of DM particles, for $\alpha = 1/30$ and $m_\chi = 1$ TeV; bottom-right: the evolution of DM abundance with the cosmic time $x \equiv m_\chi/T$ taking into account the SE corresponding to the models in the bottom-left panel.

larger, and finally reach a platform when the DM particles are cold enough. We also label the velocity dispersion of today's MW halo, $\sigma \approx 5 \times 10^{-4}$ (150 km s^{-1}). It can be inferred that if the difference of the SE between the smooth MW halo and the saturation value is larger, the boost effect from substructures should be more remarkable. We will go details on this point in Sec. V. In the bottom-right panel of Fig. 1 we show the evolution of DM abundance with the cosmic time $x \equiv m_\chi/T$ for the models with $m_\phi = 10, 19$ and 19.7 GeV shown in the bottom-left panel. We find that there is almost no difference compared with the case without SE. The annihilation cross section without SE, i.e. $\langle \sigma v \rangle_0 \approx 1.2 - 1.5 \times 10^{-26}$

$\text{cm}^3 \text{s}^{-1}$ is found to give the right relic density of DM [30] for different models.

In the following, we will employ the models shown in the bottom-left panel of Fig. 1 to discuss the effects on DM substructures from SE. These models cover the non-resonant ($m_\phi = 10$ or 1 GeV), moderately resonant ($m_\phi = 19$ or 1.24 GeV) and strongly resonant ($m_\phi = 19.7$ or 1.32 GeV) Sommerfeld enhanced cases without loss of generality. For other parameters the conclusions can be easily translated. Note that in this work we will focus on the boost factors from DM substructures. We will not go in details of the particle physical model of DM or the comparison of the expected fluxes of e^\pm and \bar{p} with the data. However, some rough implications from the observational data are adopted, like the mass of DM $m_\chi \approx 1$ TeV according to ATIC [2] or Fermi [6] results. Actually as studied in many related papers [5, 24], a DM model with $m_\chi \approx 1$ TeV and a total enhancement factor of about several hundred can reproduce the observational data. That is to say most of the chosen models as shown in the bottom-left panel of Fig. 1 (except for $m_\phi = 10$ GeV) are potential ones which can explain the data, depending on the clumpiness boost factors that will be discussed below.

III. DM DISTRIBUTION AND SUBSTRUCTURES

A. Density profile

The DM density profile based on N-body simulations can be generally parameterized as a scale-invariant form

$$\rho = \frac{\rho_s}{(r/r_s)^\gamma [1 + (r/r_s)^\alpha]^{(\beta-\gamma)/\alpha}}, \quad (4)$$

where ρ_s and r_s are the scale density and radius respectively, and (α, β, γ) are the shape parameters which can be fitted from simulations. The simulations usually favor a central cusp of the density profile, like the NFW profile with $(\alpha, \beta, \gamma) = (1, 3, 1)$ [31] and the Moore profile with $(\alpha, \beta, \gamma) = (1.5, 3, 1.5)$ [32], though the exact slope near the center is still under debate. In this work we will employ both the NFW and Moore profiles for discussion. Note that the central density for these profiles is divergent. To avoid the singularity, we introduce a maximum central density ρ_{max} due to the fact that there should be a balance between the annihilating rate and the in-fall rate of DM [33]. For typical parameter settings we have $\rho_{\text{max}} = 10^{18} \sim 10^{19} \text{ M}_\odot \text{ kpc}^{-3}$ (Paper I). Throughout this paper we fix ρ_{max} to be 10^{18} M_\odot

kpc^{-3} except special claims.

The scale parameters ρ_s and r_s are determined using the virial mass M_{vir} , and the concentration parameter c_{vir} . The virial radius of a DM halo is defined as

$$r_{\text{vir}} = \left(\frac{M_{\text{vir}}}{(4\pi/3)\Delta\rho_c} \right)^{1/3}, \quad (5)$$

where $\Delta \approx 18\pi^2 + 82x - 39x^2$ with $x = \Omega_M(z) - 1 = -\frac{\Omega_\Lambda}{\Omega_M(1+z)^3 + \Omega_\Lambda}$ (valid for Λ CDM universe, [34]) is the overdensity, and $\rho_c \approx 138M_\odot \text{kpc}^{-3}$ is the critical density of the universe. The concentration parameter c_{vir} is defined as

$$c_{\text{vir}} = \frac{r_{\text{vir}}}{r_{-2}}, \quad (6)$$

where r_{-2} refers to the radius at which $\frac{d(r^2\rho)}{dr}|_{r=r_{-2}} = 0$. The concentration parameter c_{vir} relates r_{vir} and the density profile parameter as (Paper I)

$$r_s^{\text{NFW}} = \frac{r_{\text{vir}}(M_{\text{vir}})}{c_{\text{vir}}(M_{\text{vir}})}, \quad r_s^{\text{Moore}} = \frac{r_{\text{vir}}(M_{\text{vir}})}{0.63 c_{\text{vir}}(M_{\text{vir}})}. \quad (7)$$

Therefore if the $c_{\text{vir}} - M_{\text{vir}}$ relation is specified, r_s is determined using Eq.(7). Finally we normalize the total mass $\int \rho(r)dV$ to M_{vir} to get the scale density ρ_s .

Generally the $c_{\text{vir}} - M_{\text{vir}}$ relation can be derived through fitting the observational mass profiles of gravitational systems like galaxy clusters [35, 36]. However, the observational sample is limited in a narrow mass range and prevents us from investigating the case down to very low mass haloes. Thus similar as in Paper I we will use the toy model predictions on the $c_{\text{vir}} - M_{\text{vir}}$ relation based on simulations. Two concentration models B01 [37] and ENS01 [38] are adopted for discussion, with fitted polynomial form at $z = 0$ as

$$\ln(c_{\text{vir}}) = \sum_{i=0}^4 C_i \times \left[\ln \left(\frac{M_{\text{vir}}}{M_\odot} \right) \right]^i, \quad (8)$$

with

$$C_i^{B01} = \{4.34, -0.0384, -3.91 \times 10^{-4}, -2.2 \times 10^{-6}, -5.5 \times 10^{-7}\}, \quad (9)$$

and

$$C_i^{\text{ENS01}} = \{3.14, -0.018, -4.06 \times 10^{-4}, 0, 0\}. \quad (10)$$

B. Substructures

The mass and spatial distributions of DM substructures can be parameterized as [39, 40]

$$\frac{dN_{\text{sub}}(r, M_{\text{sub}})}{dV dM_{\text{sub}}} = N_{\text{sub}} \times \frac{dP_{\text{M}}(M_{\text{sub}})}{dM_{\text{sub}}} \times \frac{dP_{\text{V}}(r)}{dV}, \quad (11)$$

where N_{sub} is the total number of subhaloes, $dP_{\text{M}}/dM_{\text{sub}}$ and dP_{V}/dV are the normalized mass and spatial distribution probabilities. For the mass function, the N-body simulations show a power law distribution

$$\frac{dP_{\text{M}}(M_{\text{sub}})}{dM_{\text{sub}}} \propto \left(\frac{M_{\text{sub}}}{M_{\odot}} \right)^{-\alpha_{\text{m}}}. \quad (12)$$

This relation is assumed to hold in a wide mass range, from the most massive subhalo in the MW, $M_{\text{max}} \sim 10^{10} M_{\odot}$, down to the scale of Earth mass $M_{\text{min}} \sim 10^{-6} M_{\odot}$ [40]. The power law index α_{m} is about 2, however, with a scattering from ~ 1.7 to ~ 2.1 in various works [18, 41, 42]. The two recent highest resolution simulations, Aquarius and Via Lactea find the values of α_{m} to be 1.9 and 2.0 respectively [43, 44]. For $\alpha_{\text{m}} \gtrsim 2.0$ the mass fraction of subhaloes will be sensitively dependent on the lower cut of the mass of subhalo, which is still very uncertain [45, 46, 47]. In this work we adopt the fiducial values of $\alpha_{\text{m}} = 1.9$ and the minimum mass $M_{\text{min}} = 10^{-6} M_{\odot}$ as benchmark model, while the results of other parameters are also given for comparison.

The spatial distribution of subhaloes is usually found to be anti-biased with respect to the DM density distribution, and can be fitted with an cored isothermal function (e.g.,[39])

$$\frac{dP_{\text{V}}(r)}{4\pi r^2 dr} \propto \left[1 + \left(\frac{r}{r_{\text{H}}} \right)^2 \right]^{-1}, \quad (13)$$

where $r_{\text{H}} \approx 0.14 r_{\text{vir}}^{\text{MW}}$ is the core radius.

The normalization of the total number of subhaloes is determined by setting the number with mass heavier than $10^8 M_{\odot}$ is 100 (Paper I). For such a normalization and the mass function slope $\alpha_{\text{m}} = 1.9$, we find the total number of subhaloes with minimum mass $M_{\text{min}} = 10^{-6} M_{\odot}$ is about 4×10^{14} , which is consistent with the one obtained in Ref. [40].

Finally, we simply give the overall property of the MW halo. We will adopt a NFW profile with total mass $M_{\text{MW}} \approx 10^{12} M_{\odot}$ [48]. The virial radius of the MW halo is about 270 kpc, and the concentration parameter calculated using B01 model is about 13.6. The local density is then calculated to be $\rho_0(r_{\odot} = 8.5 \text{ kpc}) \approx 0.25 \text{ GeV cm}^{-3}$. Note that a fraction of

mass f will be in substructures, so the actual density of the so-called “smooth” component is $(1-f)\rho(r)$. For the above benchmark configuration of subhaloes, $f \approx 0.14$ is found. Since we mainly focus on the boost factors from subhaloes, this smooth halo model is fixed in the following discussion.

IV. PROPAGATION MODEL AND BOOST FACTORS

In the Galaxy the transport of charged particles is affected by several processes. The scattering off random magnetic fields will lead to spatial and energy diffusions. The stellar wind may also blow away the cosmic rays (CRs) from the Galactic plane. In addition, interactions of CR particles with the interstellar radiation field (ISRF) and/or the interstellar medium (ISM) can result in continuous and catastrophic energy losses. Since the detailed processes affect the propagation are species-dependent, we will describe the treatments for antiprotons and positrons below respectively. The basic common framework is as follows. For the transport processes we take a spatial independent diffusion coefficient $D(E) = \beta D_0 \mathcal{R}^\delta$ (where $\mathcal{R} = pc/Ze$ is the rigidity) and a constant wind V_c directed outwards along z . CRs are confined within a cylinder halo L , i.e. the differential density, $dN/dE \equiv n$, is bound by $n(z = \pm L, R_{\max}) = 0$ with R_{\max} of the scale of the visible Galaxy¹. The free parameters of the model are the halo size L of the Galaxy, the normalization of the diffusion coefficient K_0 and its slope δ , and the constant galactic wind V_c .

The propagation equation of CRs can be generally written as

$$-D\Delta N + V_c \frac{\partial N}{\partial z} + 2h\Gamma_{\text{tot}}\delta(z)N + \frac{\partial}{\partial E} \left(\frac{dE}{dt} N \right) = q(\mathbf{x}, E), \quad (14)$$

where $\Gamma_{\text{tot}} = \sum_{i=H,He} n_i \sigma_i v$ is the destruction rate of CRs through interaction with ISM in the thin gas disk with half height $h \approx 0.1$ kpc, dE/dt is the energy loss rate, and $q(\mathbf{x}, E)$ is the source function.

Given the propagated fluxes of CRs, we then define the boost factor as the ratio of the sum of the smooth and substructure contributions to the smooth one without substructures. The detailed formula of the solutions of the propagation equations and the boost factor are presented in the Appendix. For more details please refer to Paper I and references therein.

¹ Note that the actual effective volume of CRs depends on the propagation parameters, see e.g., [49].

V. RESULTS

For the convenience of comparison, we specify the reference model configuration based on the descriptions in previous sections: $M_{\min} = 10^{-6} M_{\odot}$, $\alpha_m = 1.9$; the inner profile of subhalo is NFW, and the concentration model is B01; the propagation parameters are the median settings (see Appendix A). We also include the discussion about an extreme configuration with $\alpha_m = 2.0$, Moore inner profile and B01 concentration model. These two parameter settings are compiled in Table I.

	α_m	profile	$M_{\min}(M_{\odot})$	concentration	propagation
reference	1.9	NFW	10^{-6}	B01	MED
extreme	2.0	Moore	10^{-6}	B01	MED

TABLE I: The reference and extreme model configurations of DM substructures.

To get a rough idea about how large the enhancement due to SE is necessary to give a non-negligible boost factor, we give the relative fluxes of positrons (left) and antiprotons (right) in the absence of SE in Fig. 2. It is shown that the contribution to the charged particle fluxes of DM subhaloes for the reference configuration is about two orders of magnitude lower than the smooth component. If the inner profile of DM subhalo is as cuspy as Moore profile, the resulting contribution from DM subhaloes is still about one order of magnitude lower than the smooth one. Thus in the absence of SE case, it is very difficult to generate large enough boost factor only from DM clumpiness. More details were discussed in Paper I.

In the following we will discuss the cases including the SE. Three kinds of SE enhanced cases, i.e., the non-resonant case ($m_{\phi} = 10$ or 1 GeV of Fig. 1), the moderately resonant case ($m_{\phi} = 19$ or 1.24 GeV) and the strongly resonant case ($m_{\phi} = 19.7$ or 1.32 GeV) respectively, are discussed one by one.

A. Non-resonant case

In Figs. 3 and 4 we show the boost factors for e^+ and \bar{p} respectively, for the non-resonant SE model. For the first three panels discussing the effects of DM distribution or propagation

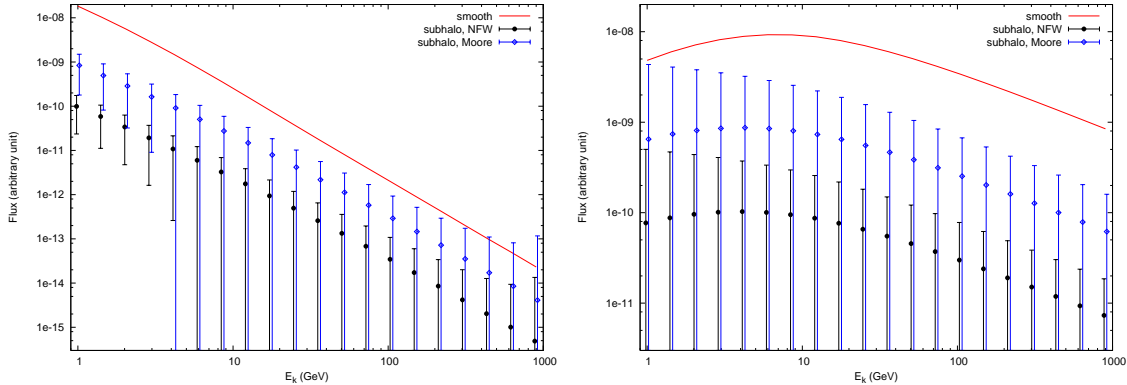


FIG. 2: The (relative) fluxes of positrons (left) and antiprotons (right) from DM annihilation for the smooth component (red solid line), the subhalo component with reference configuration (black full circle), and the subhalo component with Moore inner profile (blue empty diamond).

models we set $m_\phi = 10$ GeV. Only in the last panel we show the comparison between various values of m_ϕ . From Fig. 1 we can see that for $m_\phi = 10$ GeV, there should be no additional enhancement effect on the substructures from SE because the smooth halo has lay in the saturation region. In other words the SE enhancement factor will be the same for both the smooth component and the substructures. Therefore the results should be the same as discussed in Paper I, where we find the boost effects from DM substructures are negligible for DM distributions from N-body simulations.

For the $m_\phi = 1$ GeV case, we find a factor about 2 times larger for the saturation value than the smooth MW halo. Therefore it will lead to ~ 2 times larger boost factor than that for $m_\phi = 10$ GeV since most of the subhaloes lie in the saturation region². This can be seen from the extreme case³ in the last panels of Figs. 3 and 4.

From the Figs. 3 and 4 we have more details about the boost factor and its uncertainty.

- Energy dependence of the boost factor B .

As firstly pointed out in Ref. [20], the boost factor from DM substructures is energy dependent instead of a constant due to the energy-dependent propagation effects of charged CRs. This energy-dependent propagation can be further translated into the

² For the most massive subhalo $M_{\text{max}} = 10^{10} M_\odot$, we have $\sigma \approx 2 \times 10^{-4}$.

³ Note, however, since the boost factor is dominated by the smooth component for the reference configuration, we do not see remarkable differences between $m_\phi = 10$ and 1 GeV for the reference model.

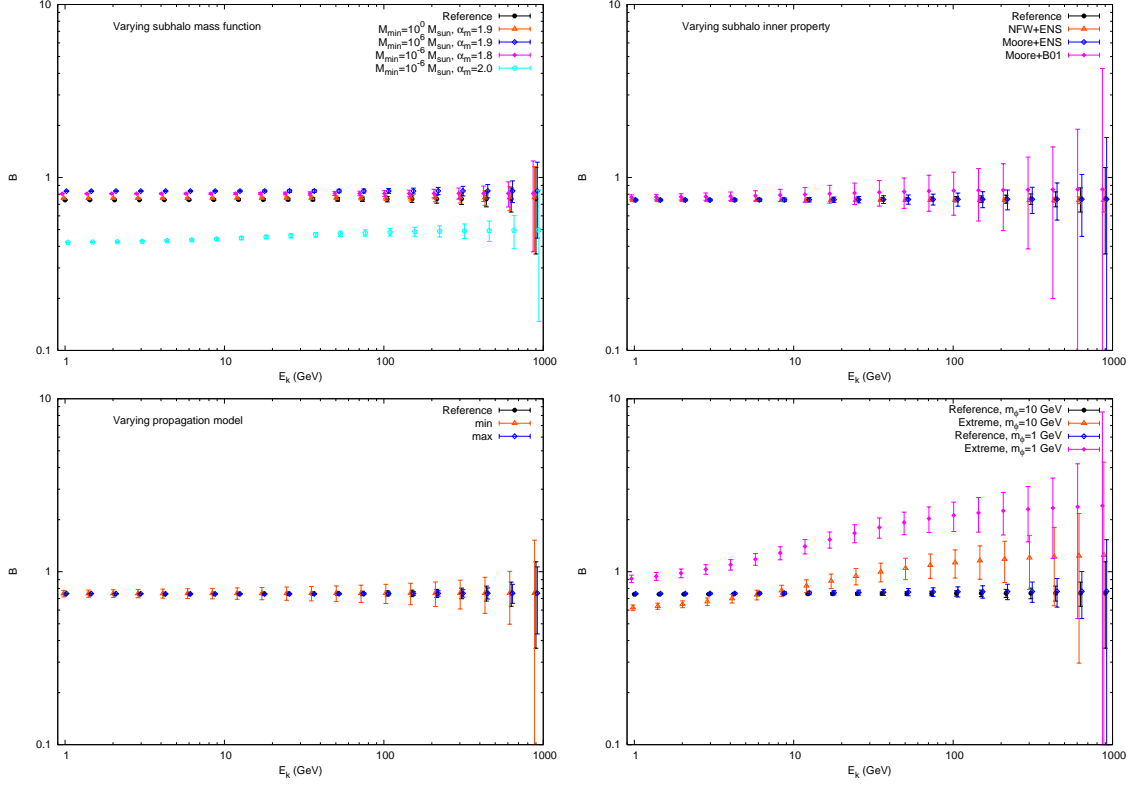


FIG. 3: The boost factors of positrons for the non-resonant SE case, for different model configurations: varying the distribution of subhalo population (top-left); varying the inner property of subhalo (top-right); varying the propagation parameters (bottom-left); and finally the extreme cases with $\alpha_m = 2.0$, Moore inner profile with B01 concentration model (bottom-right). The errorbars show the variances of the boost factors. For clarity of the plot, we slightly shift the energy axis among different models in one panel.

differences of spatial distributions between the smooth component and the substructures. This is because the effective propagation lengths of e^+ and \bar{p} vary with energy [19, 49]. Specifically, for e^+ the propagation length decreases with the increase of energy due to faster energy loss of high energy positrons; while for \bar{p} the case is just contrary. Thus we may expect a lower boost factor for low energy positrons since it reflects the ratio of substructures to the smooth halo in a larger volume, which includes more smooth contribution when closing to the GC. Similarly, for antiprotons we will expect a higher boost factor for low energy particles. These properties can be seen clearly in the bottom-right panels of Figs. 3 and 4.

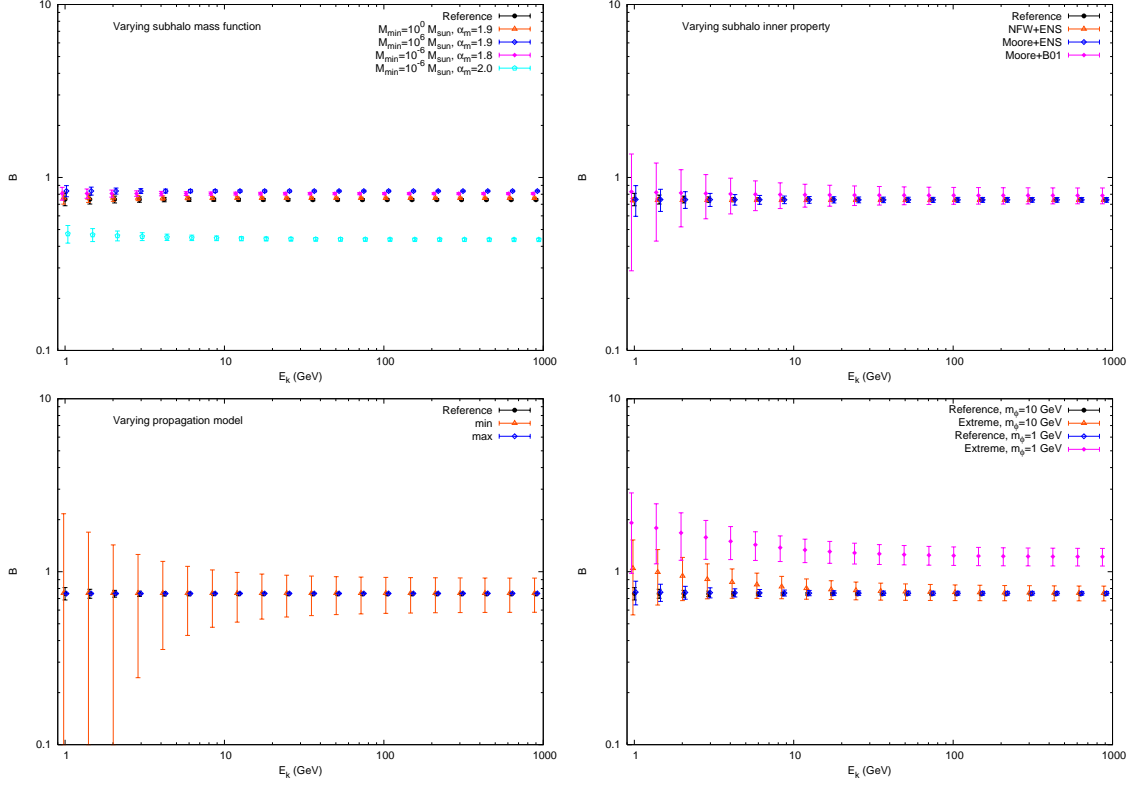


FIG. 4: The same as Fig. 3 but for antiprotons.

- Energy dependence of the variance σ_B .

The variance of the boost factor σ_B is also related to the effective propagation volume, and hence the energy, of CRs. The smaller the propagation volume, the larger the statistical uncertainty. Therefore the variance is larger for e^+ (smaller for \bar{p}) at high energies. These behaviors are also shown in Figs. 3 and 4.

- Dependence on the subhalo mass function.

Since we use the number of subhalos above $10^8 M_\odot$ to normalize the number distribution function, the lower mass cut M_{\min} and the mass function slope α_m will affect the fraction of subhalo contribution to the total signals. If M_{\min} is smaller, or α_m is larger, the mass fraction of substructures f will be larger (see Paper I). However, when the boost from subhalos is not significant a large fraction of mass in subhalos may lead to suppress of DM annihilation, as shown in the figures. This is because the boost factor approximates as $(1 - f)^2$ according to Eq.(B12).

It is not direct to derive the influence on the variance of the boost factor. From Eq.(B13) we know that $\sigma_B \propto \sigma_{\text{sub}}$ with σ_{sub} given in Eq.(B7). The variance of subhalo flux will depend on the total number of subhaloes N_{sub} , the average and variance of the annihilation luminosity ξ of a single clump. As shown in Figs. 3 and 4 (and also the related discussions in Paper I), σ_B does not depend sensitively on the parameters M_{min} and α_m .

- Dependence on the inner property of subhalo.

In the top-right panels of Figs. 3 and 4 we show the boost factors together with the variances when changing the subhalo inner profile and the concentration model. It is known that B01 concentration model would give larger annihilation luminosity ξ than ENS model, and Moore profile would also give larger flux than NFW profile. Therefore we get the largest boost factor for Moore + B01 configuration, while the smallest one for NFW + ENS configuration, although both are still negligible (~ 1). As for the variance, since the annihilation luminosity ξ for ENS concentration model or Moore profile differs from the reference model (B01, NFW) by nearly a constant factor⁴, we expect $\sigma_\xi/\langle\xi\rangle_M$ to be almost unchanged. Then from Eq.(B7) we have $\sigma_{\text{sub}} \propto \langle\Phi_{\text{sub}}\rangle$, which is the largest for Moore + B01 model and smallest for NFW + ENS model.

- Dependence on the propagation model.

The effects of various propagation parameters given in Table II are shown in the bottom-left panels of Figs. 3 and 4. Since the propagation parameters affect both the smooth component and substructures, the boost factor will not be sensitive to the propagation parameters. However, the propagation parameters will strongly affect the effective propagation length of particles ($\lambda_D^{\epsilon^+} \propto \sqrt{D_0}$, and $\lambda_D^{\bar{p}} \propto D/V_c$), and then lead to different variances. For the minimum parameter setting the effective propagation length is the smallest, so the variance is the largest.

- The *maximal* case.

We now come to the extreme model configuration with all the maximum settings of parameters discussed above, i.e., B01 concentration model, Moore inner profile and

⁴ It is weakly dependent on clump mass M_{sub} , see Fig. 3 of Paper I.

mass function slope $\alpha_m = 2.0^5$, to show the *maximal* boost factor. The median propagation model is adopted due to the fact that the boost factor does not depend on the propagation parameters sensitively. We find that in this extreme case, the *maximal* boost factor will be less than $2 \sim 3$.

B. Moderately resonant case

If the smooth halo lies out of the saturation region of SE, we may expect stronger boost effects from substructures. For the moderately resonant case with $m_\phi = 19$ GeV (or 1.24 GeV), the average SE enhancement factor for the saturation region is ~ 2 (or 4) times larger than that of the smooth MW halo. Similar with the previous discussion of $m_\phi = 1$ GeV case, we will expect $\sim 2-4$ times larger boost effect than the case without SE. Detailed calculation gives exactly the expected results, as shown in Figs. 5 and 6. The detailed properties and the parameter-dependences of B and σ_B are similar with the previous subsection. We only point out that for the extreme case (B01 + Moore + $\alpha_m = 2.0$) the boost factor is still less than, e.g. ~ 5 .

C. Strongly resonant case

The results for the strongly resonant case with $m_\phi = 19.7$ or 1.32 GeV are shown in Figs. 7 and 8. According to Fig. 1 we know that the saturation value of the SE enhancement factor is about 20 and 10^3 times larger than that of the smooth MW halo for $m_\phi = 19.7$ and 1.32 GeV respectively. For the reference model configuration, we still find almost no boost effect for $m_\phi = 19.7$ GeV. While for $m_\phi = 1.32$ GeV case the final boost factor from substructures can be as large as ~ 10 from the bottom-right panel of Figs. 7 and 8.

For the extreme case of the combinations of all maximal configurations, the *maximal* boost factor is found to be about ~ 20 and $\sim 10^3$ for $m_\phi = 19.7$ and 1.32 GeV respectively, see the bottom-right panel of Figs. 7 and 8. We also notice the variance of the extreme case is very small. This is because the main contribution comes from the very light microhalos, which have large number density. We can conclude that if the SE is finely tuned to be very

⁵ When the flux from subhaloes become to dominate the smooth component, the model with $\alpha_m = 2.0$ tends to give the larger boost factor than the one with $\alpha_m = 1.8$.

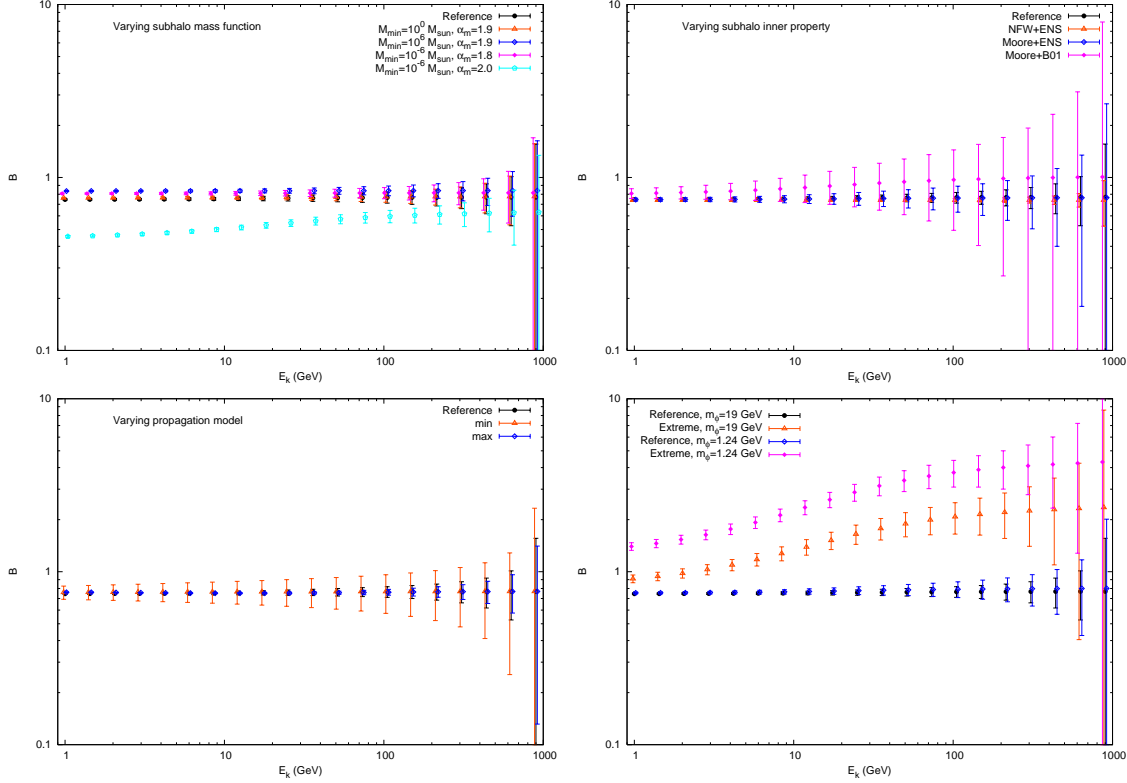


FIG. 5: The same as Fig. 3 but for the moderately resonant SE enhancement case with $m_\phi = 19$ or 1.24 GeV.

close to the resonance peak and at the same time taking very cuspy DM density profile and subhalo mass function giving huge number of microhalos, the boost effect from substructures can be remarkable. However, we think this case is not favorable. On one hand the fine tuning of the SE parameter (e.g., ϕ in this work) is needed⁶⁷. On the other hand the very cuspy subhalo density profile, like the Moore profile, is not favored by the recent high precision simulations [40, 51]. In some of these simulations the density profile is even shallower than the NFW profile [51]. We may expect in this case the boost factor due to DM clumps should be negligible no matter the SE exists or not.

⁶ If we define the degree of fine tuning as $\eta = \Delta m_\phi / m_\phi$, it is found $\eta \lesssim 1\%$ is needed to get observable boost factors.

⁷ Note also that for a very small value of m_ϕ , e.g. $m_\phi / m_\chi \lesssim 10^{-5}$, the saturation velocity can be of the order m_ϕ / m_χ [50], which may lead to a non-negligible boost factor even for the non-resonant case. However, this can be regarded as another kind of fine tuning.

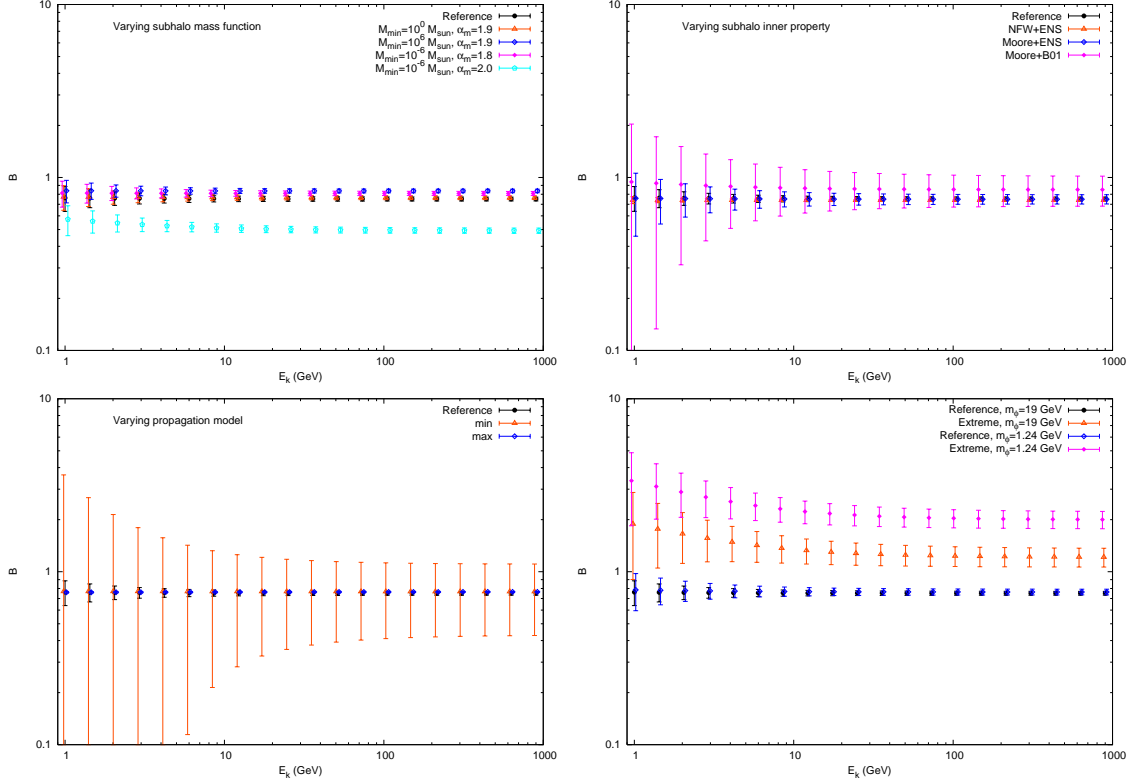


FIG. 6: The same as Fig. 5 but for antiprotons.

VI. SUMMARY AND DISCUSSION

It has been shown that the DM clumpiness in the MW halo do not tend to enhance the local observed fluxes of charged antiparticles such as antiprotons and positrons, according to the N-body simulations of DM structure formation (Paper I). In this work we re-investigate this problem taking into account the additional boost effects in DM subhaloes from the SE.

We find that generally the SE, if exists, has the same enhancement effect on the smooth component and the substructures due to the saturation behavior, except for finely tuning the SE parameter to some extreme cases when the saturation velocity is much smaller than the velocity dispersion of the smooth halo. Therefore for most cases, the conclusions of the boost factors from DM clumpiness are similar with Paper I. For the moderately resonant case like $m_\phi = 19$ or 1.24 GeV in Fig. 1, the SE enhancement factor for substructures with respect to the smooth halo is also small. The total boost factors from DM subhaloes are also negligible for the general cases of the subhalo model (mass function slope $\alpha_m \lesssim 2.0$, B01 concentration model, NFW or Moore inner density profile) given in simulations, as shown

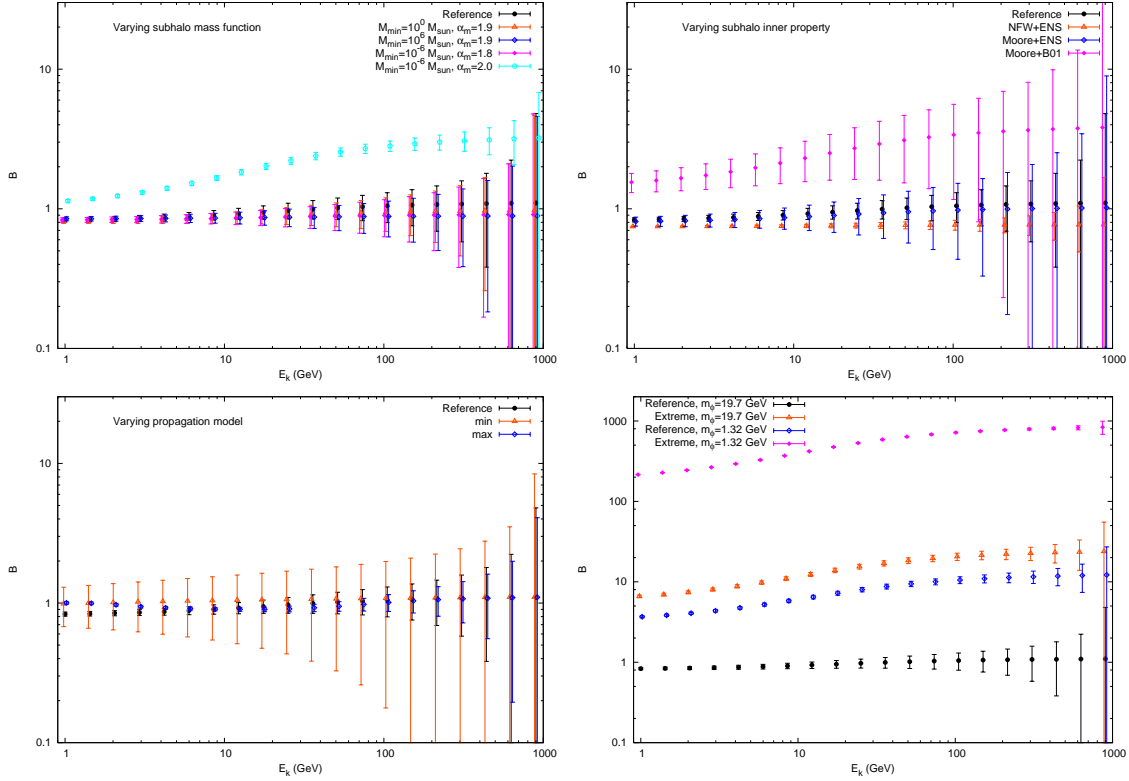


FIG. 7: The same as Fig. 3 but for strongly resonant case $m_\phi = 19.7$ or 1.32 GeV.

in the upper panels of Figs. 5 and 6. Even for the combinations of several extreme aspects of subhalo configurations, e.g., B01 concentration + Moore inner profile + $\alpha_m = 2.0$, the boost factor is as large as several.

For the strongly resonant case, e.g. $m_\phi = 19.7$ or 1.32 GeV, the additional enhancement factor for substructures from SE is much larger. Even so, for the reference configuration of DM distribution which is favored by simulations, we find the total boost factors will be less than ~ 10 . The largest boost factors for the very extreme case of subhalo configurations (B01 concentration + Moore inner profile + $\alpha_m = 2.0$) can be about ~ 10 to at most $\sim 10^3$, depending on the SE parameter adoption.

Finally we simply address the implications of DM indirect searches in the GC. As we have shown, in general cases the substructures do not play a significant role for the enhancement of DM annihilation in the solar neighborhood, as required by the PAMELA and ATIC data. Therefore, if the DM interpretation of the observational data is correct, the enhancement to the annihilation rate of local DM seems also hold for the GC if there are no other spatial

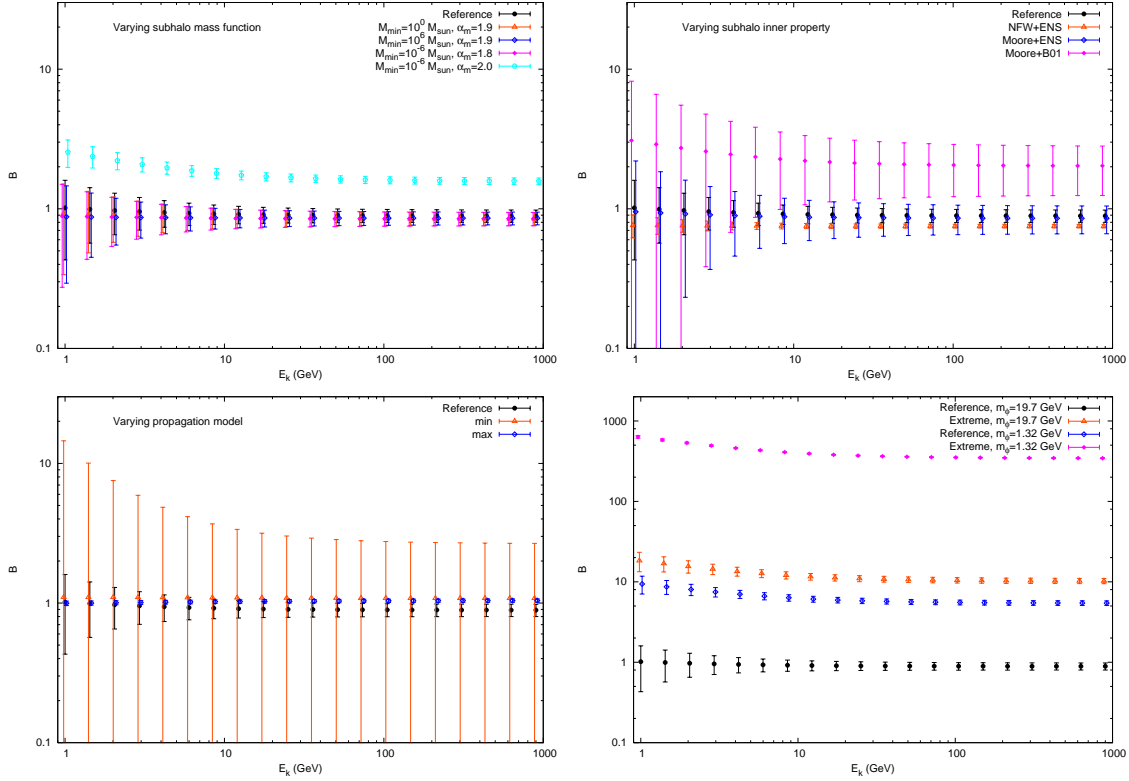


FIG. 8: The same as Fig. 7 but for antiprotons.

dependent enhancement mechanisms. Thus the photon emission from the GC will be a powerful tool to cross check the self-consistency of the theory and constrain the DM density in the GC. Alternatively, since the radio and γ -ray emission from the GC in DM annihilation scenario is strongly constrained by the observational data [23, 24, 25, 26], it may imply an appeal for a non-negligible contribution to the local DM annihilation from the clumpiness, although the DM substructures alone can not fully account for the needed large cross section.

APPENDIX A: SOLUTIONS OF THE PROPAGATION EQUATIONS OF POSITRONS AND ANTIPROTONS

1. Antiprotons

It has been shown that for the propagation of antiprotons neglecting the continuous energy losses and reacceleration can provide a good enough approach, especially for energies higher than several GeV [52]. We will also adopt this approximation here. Therefore the

relevant processes include the diffusion, convection and the catastrophic losses — inelastic scattering and annihilation in interactions. The propagation equation is

$$-D\Delta N + V_c \frac{\partial N}{\partial z} + 2h\Gamma_{\text{tot}}\delta(z)N = q(\mathbf{x}, E), \quad (\text{A1})$$

where $\Gamma_{\text{tot}} = \sum_{i=H,He} n_i \sigma_i^{\bar{p}} v$ is the destruction rate of antiprotons in the thin gas disk with half height $h \approx 0.1$ kpc [52], $q(\mathbf{x}, E)$ is the source function. The propagator for a point source located at \mathbf{x}_S , expressed in cylindrical coordinates (r, z) (symmetric in θ) is [52]

$$\mathcal{G}_{\odot}^{\bar{p}}(r, z, E) = \frac{\exp(-k_v z)}{2\pi DL} \times \sum_{n=0}^{\infty} c_n^{-1} K_0 \left(r \sqrt{k_n^2 + k_v^2} \right) \sin(k_n L) \sin[k_n(L - z)], \quad (\text{A2})$$

where r and z are the radial distance and vertical height of the source, $K_0(x)$ is the modified Bessel function of the second type, $k_v = V_c/2D$, and k_n is the solution of the equation $2k_n \cos(k_n L) = -(2h\Gamma_{\text{tot}}/D + 2k_v) \sin(k_n L)$, and $c_n = 1 - \frac{\sin(k_n L) \cos(k_n L)}{k_n L}$. For any source function $q(r, z, \theta; E)$, the local observed flux is

$$\Phi_{\odot}^{\bar{p}}(E) = \frac{v}{4\pi} \times 2 \int_0^L dz \int_0^{R_{\text{max}}} r dr \mathcal{G}_{\odot}^{\bar{p}}(r, z, E) \int_0^{2\pi} d\theta q(r, z, \theta; E). \quad (\text{A3})$$

2. Positrons

For positrons the case is some different from antiprotons. The dominant process in the propagation of positrons is energy loss due to synchrotron and inverse Compton scattering for energies higher than $\sim \text{GeV}$. In this paper we will neglect the convection and reacceleration of positrons, which is shown to be of little effect for $E \gtrsim 10$ GeV (also the interested energy range here) [53]. Then the propagation equation is

$$-D\Delta N + \frac{\partial}{\partial E} \left(\frac{dE}{dt} N \right) = q(\mathbf{x}, E), \quad (\text{A4})$$

in which the second term in the left hand side represents the energy losses. The energy loss rate of positrons due to synchrotron and inverse Compton scattering in the MW can be adopted as $dE/dt = -\epsilon^2/\tau_E$, with $\epsilon = E/1$ GeV and $\tau_E \approx 10^{16}$ s [54]. We directly write down the propagator for a point source located at (r, z) from the solar location with monochromatic injection energy E_S [19, 20]

$$\mathcal{G}_{\odot}^{e^+}(r, z, E \leftarrow E_S) = \frac{\tau_E}{E\epsilon} \times \hat{\mathcal{G}}_{\odot}(r, z, \hat{r}), \quad (\text{A5})$$

in which we define a pseudo time $\hat{\tau}$ as

$$\hat{\tau} = \tau_E \frac{\epsilon^{\delta-1} - \epsilon_S^{\delta-1}}{1 - \delta}. \quad (\text{A6})$$

$\hat{\mathcal{G}}_{\odot}(r, z, \hat{\tau})$ is the Green's function for the re-arranged diffusion equation with respect to the pseudo time $\hat{\tau}$

$$\hat{\mathcal{G}}_{\odot}(r, z, \hat{\tau}) = \frac{\theta(\hat{\tau})}{4\pi D_0 \hat{\tau}} \exp\left(-\frac{r^2}{4D_0 \hat{\tau}}\right) \times \mathcal{G}^{1D}(z, \hat{\tau}). \quad (\text{A7})$$

The effect of boundaries along $z = \pm L$ appears in \mathcal{G}^{1D} only. Following Ref. [20] we use two distinct regimes to approach \mathcal{G}^{1D} :

- for $\zeta \equiv L^2/4D_0\hat{\tau} \gg 1$ (the extension of electron sphere $\lambda \equiv \sqrt{4D_0\hat{\tau}}$ is small)

$$\mathcal{G}^{1D}(z, \hat{\tau}) = \sum_{n=-\infty}^{\infty} (-1)^n \frac{\theta(\hat{\tau})}{\sqrt{4\pi D_0 \hat{\tau}}} \exp\left(-\frac{z_n^2}{4D_0 \hat{\tau}}\right), \quad (\text{A8})$$

where $z_n = 2Ln + (-1)^n z$;

- otherwise

$$\mathcal{G}^{1D}(z, \hat{\tau}) = \frac{1}{L} \sum_{n=1}^{\infty} [\exp(-D_0 k_n^2 \hat{\tau}) \phi_n(0) \phi_n(z) + \exp(-D_0 k'_n{}^2 \hat{\tau}) \phi'_n(0) \phi'_n(z)], \quad (\text{A9})$$

where

$$\phi_n(z) = \sin[k_n(L - |z|)]; \quad k_n = (n - 1/2)\pi/L, \quad (\text{A10})$$

$$\phi'_n(z) = \sin[k'_n(L - z)]; \quad k'_n = n\pi/L. \quad (\text{A11})$$

For any source function $q(r, z, \theta; E_S)$ the local observed flux of positrons can be written as

$$\Phi_{\odot}^{e^+} = \frac{v}{4\pi} \times 2 \int_0^L dz \int_0^{R_{\max}} r dr \int_E^{\infty} dE_S \mathcal{G}_{\odot}^{e^+}(r, z, E \leftarrow E_S) \int_0^{2\pi} d\theta q(r, z, \theta; E_S). \quad (\text{A12})$$

3. Propagation parameters

The propagation parameters are determined by fitting the local observed CR spectra such as the B/C ratio and unstable-stable isotope ratio. In Ref. [55] the authors showed that there are strong degeneracies between parameters to recover the local measured B/C ratio. In this work we adopt three typical settings of parameters which are consistent with the B/C data, but give very different primary anti-particle fluxes from DM annihilation [56]. These parameters, labelled as “max”, “med” and “min” according to the primary antiparticle fluxes, are gathered in Table II.

δ	D_0 (kpc ² Myr ⁻¹)	L (kpc)	V_c (km s ⁻¹)
max 0.46	0.0765	15	5.0
med 0.70	0.0112	4	12.0
min 0.85	0.0016	1	13.5

TABLE II: Propagation parameters which are compatible with B/C analysis while giving the maximal, median and minimal anti-particle DM fluxes.

APPENDIX B: BOOST FACTORS

In this section, we calculate the fluxes of charged anti-particles and the corresponding boost factors. The source function of antiprotons and positrons from DM annihilation can be written as

$$q(\mathbf{x}, E) = \frac{\langle \sigma v \rangle}{2m_\chi^2} \frac{dN}{dE} \rho^2(\mathbf{x}), \quad (\text{B1})$$

where m_χ is the mass of DM particle which is set to be ~ 1 TeV in light of the recent observations of ATIC [2] and Fermi [6], $\langle \sigma v \rangle$ is the thermally averaged velocity weighted cross section, and dN/dE is the yield spectrum of \bar{p} or e^+ per pair annihilation. As discussed in Sec. II, the cross section is velocity-dependent if the SE is taken into account.

Then we can rewrite the fluxes of \bar{p} and e^+ , Eqs.(A3) and (A12), for the smooth halo as

$$\Phi_{\text{sm}}(E) = \frac{v}{4\pi} \times A \times \int d^3\mathbf{x} \rho_{\text{sm}}^2(\mathbf{x}) \tilde{\mathcal{G}}(r, z, E) \bar{S}(\sigma), \quad (\text{B2})$$

where $A = \langle \sigma v \rangle_0 / 2m_\chi^2$, $\bar{S}(\sigma)$ is the average SE enhancement factor, and $\tilde{\mathcal{G}}$ is the pseudo propagator (Paper I) which absorbs the source energy spectrum dN/dE in the propagator of Eq.(A2) or (A5)

$$\tilde{\mathcal{G}}^{\bar{p}}(r, z, E) = \frac{dN}{dE} \times \mathcal{G}_\odot^{\bar{p}}(r, z, E), \quad (\text{B3})$$

$$\tilde{\mathcal{G}}^{e^+}(r, z, E) = \int_E^\infty dE_S \frac{dN}{dE_S} \times \mathcal{G}_\odot^{e^+}(r, z, E \leftarrow E_S). \quad (\text{B4})$$

Note that in Eq.(B2), the SE factor should be spatially dependent due to different velocity dispersion of DM particles in the MW. Since the charged particles are thought to come from places not very far from us, we will use $\sigma_\odot \approx 150$ km s⁻¹ to represent the average velocity dispersion of the smooth DM halo for simplicity.

In our discussion we simplify the source spectrum dN/dE as in Paper I: for \bar{p} we adopt $dN/dE = 1 \text{ GeV}^{-1}$, while for e^+ we set $dN/dE = \delta(E - m_\chi)$. This adoption makes the following discussion independent of detailed particle physics model of DM, while the major property about the boost factor is still kept. It will be easy to convolve any model predicted DM source spectrum on these results.

The flux from DM subhaloes is thought to be the sum of the population of DM point sources

$$\Phi_{\text{sub}} = \sum_{i=1}^{N_{\text{sub}}} \Phi_i = \frac{vA}{4\pi} \sum_{i=1}^{N_{\text{sub}}} \xi_i \times \tilde{\mathcal{G}}(r_i, z_i, E), \quad (\text{B5})$$

where $\xi_i \equiv \int d^3\mathbf{x}' \rho^2(\mathbf{x}') \bar{S}(\sigma_i)$ is the annihilation luminosity of the i th subhalo. For the velocity dispersion of subhaloes, we adopt the relation $\sigma = 2.7 \times (M_{\text{sub}}/10^6 M_\odot)^{1/3} \text{ km s}^{-1}$ [22], with the normalization fitted from the observational results of dwarf spheroidals in Ref. [57].

Because we do not know exactly the location and mass of any specified subhalo, there should be uncertainty of the prediction of flux from subhaloes. The average and relative variance of the flux due to different realization of substructure distribution are (Paper I)

$$\langle \Phi_{\text{sub}} \rangle = N_{\text{sub}} \times \frac{vA}{4\pi} \times \langle \xi \rangle_M \times \langle \tilde{\mathcal{G}} \rangle_V, \quad (\text{B6})$$

$$\frac{\sigma_{\text{sub}}^2}{\langle \Phi_{\text{sub}} \rangle^2} = \frac{1}{N_{\text{sub}}} \left(\frac{\sigma_{\tilde{\mathcal{G}}}^2}{\langle \tilde{\mathcal{G}} \rangle_V^2} + \frac{\sigma_\xi^2}{\langle \xi \rangle_M^2} + \frac{\sigma_{\tilde{\mathcal{G}}}^2}{\langle \tilde{\mathcal{G}} \rangle_V^2} \times \frac{\sigma_\xi^2}{\langle \xi \rangle_M^2} \right), \quad (\text{B7})$$

where

$$\langle \xi \rangle_M = \int_{M_{\text{min}}}^{M_{\text{max}}} dM_{\text{sub}} \xi(M_{\text{sub}}) \frac{dP_M}{dM_{\text{sub}}}, \quad (\text{B8})$$

$$\langle \tilde{\mathcal{G}} \rangle_V = \int_V d^3\mathbf{x} \tilde{\mathcal{G}} \frac{dP_V}{dV}, \quad (\text{B9})$$

$$\sigma_\xi^2 = \int_{M_{\text{min}}}^{M_{\text{max}}} dM_{\text{sub}} \xi^2(M_{\text{sub}}) \frac{dP_M}{dM_{\text{sub}}} - \langle \xi \rangle_M^2, \quad (\text{B10})$$

$$\sigma_{\tilde{\mathcal{G}}}^2 = \int_V d^3\mathbf{x} \tilde{\mathcal{G}}^2 \frac{dP_V}{dV} - \langle \tilde{\mathcal{G}} \rangle_V^2. \quad (\text{B11})$$

Finally the boost factor, defined as the ratio of the sum of the smooth and substructure contributions to the smooth one without substructures, is⁸

$$B = \frac{\Phi_{\text{sm}} + \Phi_{\text{sub}}}{\Phi_{\text{sm}}^0} = (1 - f)^2 (1 + \Phi_{\text{sub}}/\Phi_{\text{sm}}), \quad (\text{B12})$$

⁸ Note the definition of Φ_{sm} is a bit different from Paper I, where the smooth contribution without substructures is labelled Φ_{sm} .

where Φ_{sm}^0 is the smooth contribution without substructures, and f is the mass fraction of subhaloes. The variance of the boost factor is

$$\sigma_B = \frac{\sigma_{\text{sub}}}{\Phi_{\text{sm}}^0} = (1 - f)^2 \frac{\sigma_{\text{sub}}}{\Phi_{\text{sm}}}. \quad (\text{B13})$$

ACKNOWLEDGMENTS

We thank J. Lavalle for helpful discussions on the electron/positron propagation. This work was supported in part by the Natural Sciences Foundation of China (Nos. 10773011, 10775001, 10635030) and by the Chinese Academy of Sciences under the grant No. KJCX3-SYW-N2.

-
- [1] O. Adriani *et al.*, Nature **458**, 607 (2009) [arXiv:0810.4995 [astro-ph]].
- [2] J. Chang *et al.*, Nature **456**, 362 (2008).
- [3] S. Torii *et al.*, arXiv:0809.0760 [astro-ph].
- [4] D. Hooper, P. Blasi and P. D. Serpico, JCAP **0901**, 025 (2009) [arXiv:0810.1527 [astro-ph]]; H. Yuksel, M. D. Kistler and T. Stanev, Phys. Rev. Lett. **103**, 051101 (2009) [arXiv:0810.2784 [astro-ph]]; S. Profumo, arXiv:0812.4457 [astro-ph]; K. Ioka, arXiv:0812.4851 [astro-ph]; H. B. Hu, Q. Yuan, B. Wang, C. Fan, J. L. Zhang and X. J. Bi, Astrophys. J. **700**, L170 (2009). [arXiv:0901.1520 [astro-ph]]; N. J. Shaviv, E. Nakar and T. Piran, Phys. Rev. Lett. **103**, 111302 (2009) [arXiv:0902.0376 [astro-ph.HE]]; P. Blasi, Phys. Rev. Lett. **103**, 051104 (2009) [arXiv:0903.2794 [astro-ph.HE]]; N. Kawanaka, K. Ioka and M. M. Nojiri, arXiv:0903.3782 [astro-ph.HE]; Y. Fujita, K. Kohri, R. Yamazaki, K. Ioka, Phys. Rev. D **80**, 063003 (2009) [arXiv:0903.5298 [astro-ph.HE]].
- [5] L. Bergstrom, T. Bringmann and J. Edsjo, Phys. Rev. D **78**, 103520 (2008) [arXiv:0808.3725 [astro-ph]]; V. Barger, W. Y. Keung, D. Marfatia and G. Shaughnessy, Phys. Lett. B **672**, 141 (2009) [arXiv:0809.0162 [hep-ph]]; M. Cirelli, M. Kadastik, M. Raidal and A. Strumia, Nucl. Phys. B **813**, 1 (2009) [arXiv:0809.2409 [hep-ph]]; C. R. Chen and F. Takahashi, JCAP **0902**, 004 (2009) [arXiv:0810.4110 [hep-ph]]; A. E. Nelson and C. Spitzer, arXiv:0810.5167 [hep-ph]; I. Cholis, D. P. Finkbeiner, L. Goodenough and N. Weiner, arXiv:0810.5344 [astro-ph]; Y. Nomura and J. Thaler, Phys. Rev. D **79**, 075008 (2009) [arXiv:0810.5397 [hep-ph]].

- D. Feldman, Z. Liu and P. Nath, Phys. Rev. D **79**, 063509 (2009) [arXiv:0810.5762 [hep-ph]]; P. F. Yin, Q. Yuan, J. Liu, J. Zhang, X. J. Bi, S. H. Zhu, and X. M. Zhang, Phys. Rev. D **79**, 023512 (2009) [arXiv:0811.0176 [hep-ph]]; K. Ishiwata, S. Matsumoto and T. Moroi, Phys. Lett. B **675**, 446 (2009) [arXiv:0811.0250 [hep-ph]]; P. J. Fox and E. Poppitz, Phys. Rev. D **79**, 083528 (2009) [arXiv:0811.0399 [hep-ph]]; C. R. Chen, F. Takahashi and T. T. Yanagida, Phys. Lett. B **673**, 255 (2009) [arXiv:0811.0477 [hep-ph]]; K. Hamaguchi, E. Nakamura, S. Shirai and T. T. Yanagida, Phys. Lett. B **674**, 299 (2009) [arXiv:0811.0737 [hep-ph]]; E. Ponton and L. Randall, JHEP **0904**, 080 (2009) [arXiv:0811.1029 [hep-ph]]; A. Ibarra and D. Tran, JCAP **0902**, 021 (2009) [arXiv:0811.1555 [hep-ph]]; C. R. Chen, F. Takahashi and T. T. Yanagida, Prog. Theor. Phys. **122**, 553 (2009) [arXiv:0811.3357 [astro-ph]]; I. Cholis, G. Dobler, D. P. Finkbeiner, L. Goodenough and N. Weiner, arXiv:0811.3641 [astro-ph]; E. Nardi, F. Sannino and A. Strumia, JCAP **0901**, 043 (2009) [arXiv:0811.4153 [hep-ph]]; J. Liu, P. F. Yin and S. H. Zhu, Phys. Rev. D **79**, 063522 (2009) [arXiv:0812.0964 [astro-ph]]; R. Allahverdi, B. Dutta, K. Richardson-McDaniel and Y. Santoso, Phys. Rev. D **79**, 075005 (2009) [arXiv:0812.2196 [hep-ph]]; K. Hamaguchi, S. Shirai and T. T. Yanagida, Phys. Lett. B **673**, 247 (2009) [arXiv:0812.2374 [hep-ph]]; X. J. Bi, P. H. Gu, T. Li and X. Zhang, JHEP **0904**, 103 (2009) [arXiv:0901.0176 [hep-ph]]; S. Khalil, H. S. Lee and E. Ma, Phys. Rev. D **79**, 041701R (2009) [arXiv:0901.0981 [hep-ph]]; Q. H. Cao, E. Ma and G. Shaughnessy, Phys. Lett. B **673**, 152 (2009) [arXiv:0901.1334 [hep-ph]]; F. Takahashi and E. Komatsu, arXiv:0901.1915 [astro-ph]; C. H. Chen, C. Q. Geng and D. V. Zhuridov, Phys. Lett. B **675**, 77 (2009) [arXiv:0901.2681 [hep-ph]]; P. Meade, M. Papucci and T. Volansky, arXiv:0901.2925 [hep-ph]; J. Mardon, Y. Nomura, D. Stolarski and J. Thaler, JCAP **0905**, 016 (2009) [arXiv:0901.2926 [hep-ph]]; D. Hooper and K. Zurek, Phys. Rev. D **79**, 103529 (2009) [arXiv:0902.0593 [hep-ph]]; K. Cheung, P. Y. Tseng and T. C. Yuan, Phys. Lett. B **678**, 293 (2009) [arXiv:0902.4035 [hep-ph]]; S. L. Chen, R. N. Mohapatra, S. Nussinov and Y. Zhang, Phys. Lett. B **677**, 311 (2009) [arXiv:0903.2562 [hep-ph]].
- [6] A. A. Abdo *et al.* [The Fermi LAT Collaboration], Phys. Rev. Lett. **102**, 181101 (2009) [arXiv:0905.0025 [astro-ph.HE]].
- [7] L. Bergstrom, J. Edsjo and G. Zaharijas, Phys. Rev. Lett. **103**, 031103 (2009) [arXiv:0905.0333 [astro-ph.HE]]; D. Grasso *et al.*, Astropart. Phys. **32**, 140 (2009) [arXiv:0905.0636 [astro-ph.HE]].

- [8] D. Hooper, A. Stebbins and K. M. Zurek, Phys. Rev. D **79**, 103513 (2009) [arXiv:0812.3202 [hep-ph]].
- [9] T. Bringmann, J. Lavalle and P. Salati, Phys. Rev. Lett. **103**, 161301 (2009) [arXiv:0902.3665 [astro-ph.CO]].
- [10] P. Brun, T. Delahaye, J. Diemand, S. Profumo and P. Salati, Phys. Rev. D **80**, 035023 (2009) [arXiv:0904.0812 [astro-ph.HE]].
- [11] W. B. Lin, D. H. Huang, X. Zhang and R. H. Brandenberger, Phys. Rev. Lett. **86**, 954 (2001) [arXiv:astro-ph/0009003]; R. Jeannerot, X. Zhang and R. H. Brandenberger, JHEP **9912**, 003 (1999) [arXiv:hep-ph/9901357]; X. J. Bi, R. Brandenberger, P. Gondolo, T. J. Li, Q. Yuan and X. M. Zhang, Phys. Rev. D **80**, 103502 (2009) [arXiv:0905.1253 [hep-ph]].
- [12] J. Hisano, S. Matsumoto, M. M. Nojiri and O. Saito, Phys. Rev. D **71**, 063528 (2005) [arXiv:hep-ph/0412403]; J. Hisano, S. Matsumoto, M. Nagai, O. Saito and M. Senami, Phys. Lett. B **646**, 34 (2007) [arXiv:hep-ph/0610249].
- [13] M. Cirelli, A. Strumia and M. Tamburini, Nucl. Phys. B **787**, 152 (2007) [arXiv:0706.4071 [hep-ph]].
- [14] N. Arkani-Hamed, D. P. Finkbeiner, T. R. Slatyer and N. Weiner, Phys. Rev. D **79**, 015014 (2009) [arXiv:0810.0713 [hep-ph]].
- [15] M. Pospelov and A. Ritz, Phys. Lett. B **671**, 391 (2009) [arXiv:0810.1502 [hep-ph]].
- [16] M. Lattanzi and J. I. Silk, Phys. Rev. D **79**, 083523 (2009) [arXiv:0812.0360 [astro-ph]].
- [17] M. Ibe, H. Murayama and T. T. Yanagida, Phys. Rev. D **79**, 095009 (2009) [arXiv:0812.0072 [hep-ph]]; W. L. Guo and Y. L. Wu, Phys. Rev. D **79**, 055012 (2009) [arXiv:0901.1450 [hep-ph]]; X. J. Bi, X. G. He and Q. Yuan, Phys. Lett. B **678**, 168 (2009) [arXiv:0903.0122 [hep-ph]].
- [18] G. Tormen, A. Diaferio and D. Syer, Mon. Not. Roy. Astron. Soc. **299**, 728 (1998); A. A. Klypin, S. Gottlober and A. V. Kravtsov, Astrophys. J. **516**, 530 (1999) [arXiv:astro-ph/9708191]; B. Moore, S. Ghigna, F. Governato, G. Lake, T. Quinn, J. Stadel and P. Tozzi, Astrophys. J. **524** (1999) L19 CITATION = ASJOA,524,L19; S. Ghigna, B. Moore, F. Governato, G. Lake, T. Quinn and J. Stadel, Astrophys. J. **544**, 616 (2000) [arXiv:astro-ph/9910166]; A. R. Zentner and J. S. Bullock, Astrophys. J. **598**, 49 (2003) [arXiv:astro-ph/0304292]; G. De Lucia *et al.*, Mon. Not. Roy. Astron. Soc. **348**, 333 (2004) [arXiv:astro-ph/0306205];
- [19] J. Lavalle, Q. Yuan, D. Maurin and X. J. Bi, Astron. Astrophys. **479**, 427 (2008).

- [arXiv:0709.3634 [astro-ph]] (Paper I).
- [20] J. Lavalley, J. Pochon, P. Salati and R. Taillet, *Astron. Astrophys.* **462**, 827 (2007).
[arXiv:astro-ph/0603796].
- [21] L. Pieri, M. Lattanzi and J. Silk, arXiv:0902.4330 [astro-ph.HE].
- [22] J. Bovy, *Phys. Rev. D* **79**, 083539 (2009) [arXiv:0903.0413 [astro-ph.HE]].
- [23] G. Bertone, M. Cirelli, A. Strumia and M. Taoso, *JCAP* **0903**, 009 (2009) [arXiv:0811.3744 [astro-ph]].
- [24] J. Zhang, X. J. Bi, J. Liu, S. M. Liu, P. F. Yin, Q. Yuan and S. H. Zhu, *Phys. Rev. D* **80**, 023007 (2009) [arXiv:0812.0522 [astro-ph]].
- [25] L. Bergstrom, G. Bertone, T. Bringmann, J. Edsjo and M. Taoso, *Phys. Rev. D* **79**, 081303 (2009) [arXiv:0812.3895 [astro-ph]].
- [26] M. Cirelli and P. Panci, *Nucl. Phys. B* **821**, 399 (2009) [arXiv:0904.3830 [astro-ph.CO]].
- [27] R. Iengo, *JHEP* **0905**, 024 (2009) [arXiv:0902.0688 [hep-ph]]; R. Iengo, arXiv:0903.0317 [hep-ph].
- [28] S. Cassel, arXiv:0903.5307 [hep-ph].
- [29] B. Robertson and A. Zentner, *Phys. Rev. D* **79**, 083525 (2009) [arXiv:0902.0362 [astro-ph.CO]].
- [30] E. Komatsu *et al.* [WMAP Collaboration], *Astrophys. J. Suppl.* **180**, 330 (2009) [arXiv:0803.0547 [astro-ph]].
- [31] J. F. Navarro, C. S. Frenk and S. D. M. White, *Astrophys. J.* **490**, 493 (1997).
- [32] B. Moore, T. R. Quinn, F. Governato, J. Stadel and G. Lake, *Mon. Not. Roy. Astron. Soc.* **310**, 1147 (1999) [arXiv:astro-ph/9903164].
- [33] V. S. Berezinsky, A. V. Gurevich and K. P. Zybin, *Phys. Lett. B* **294**, 221 (1992).
- [34] G. L. Bryan and M. L. Norman, *Astrophys. J.* **495**, 80 (1998) [arXiv:astro-ph/9710107].
- [35] D. A. Buote, F. Gastaldello, P. J. Humphrey, L. Zappacosta, J. S. Bullock, F. Brighenti and W. G. Mathews, *Astrophys. J.* **664**, 123 (2007).
- [36] J. M. Comerford and P. Natarajan, *Mon. Not. Roy. Astron. Soc.* **379**, 190 (2007).
- [37] J. S. Bullock *et al.*, *Mon. Not. Roy. Astron. Soc.* **321**, 559 (2001).
- [38] V. R. Eke, J. F. Navarro and M. Steinmetz, *Astrophys. J.* **554**, 114 (2001).
- [39] J. Diemand, B. Moore and J. Stadel, *Mon. Not. Roy. Astron. Soc.* **352**, 535 (2004).
- [40] J. Diemand, B. Moore and J. Stadel, *Nature* **433**, 389 (2005).
- [41] L. Gao, S. D. M. White, A. Jenkins, F. Stoehr and V. Springel, *Mon. Not. Roy. Astron. Soc.*

- 355**, 819 (2004) [arXiv:astro-ph/0404589].
- [42] L. Shaw, J. Weller, J. P. Ostriker and P. Bode, *Astrophys. J.* **646**, 815 (2006).
- [43] J. Diemand, M. Kuhlen and P. Madau, *Astrophys. J.* **657**, 262 (2007) [arXiv:astro-ph/0611370].
- [44] V. Springel *et al.*, *Mon. Not. Roy. Astron. Soc.* **391**, 1685 (2008) [arXiv:0809.0898 [astro-ph]].
- [45] V. Berezhinsky, V. Dokuchaev and Y. Eroshenko, *Phys. Rev. D* **68**, 103003 (2003) [arXiv:astro-ph/0301551].
- [46] A. M. Green, S. Hofmann and D. J. Schwarz, *Mon. Not. Roy. Astron. Soc.* **353**, L23 (2004) [arXiv:astro-ph/0309621].
- [47] S. Profumo, K. Sigurdson and M. Kamionkowski, *Phys. Rev. Lett.* **97**, 031301 (2006) [arXiv:astro-ph/0603373].
- [48] X. X. Xue *et al.* [SDSS Collaboration], *Astrophys. J.* **684**, 1143 (2008) [arXiv:0801.1232 [astro-ph]].
- [49] D. Maurin and R. Taillet, *Astron. Astrophys.* **404**, 949 (2003) [arXiv:astro-ph/0212113].
- [50] M. Kuhlen and D. Malyshev, *Phys. Rev. D* **79**, 123517 (2009) [arXiv:0904.3378 [hep-ph]].
- [51] J. F. Navarro *et al.*, *Mon. Not. Roy. Astron. Soc.* **349**, 1039 (2004) [arXiv:astro-ph/0311231]; D. Merritt, J. F. Navarro, A. Ludlow and A. Jenkins, *Astrophys. J.* **624**, L85 (2005) [arXiv:astro-ph/0502515]; A. W. Graham, D. Merritt, B. Moore, J. Diemand and B. Terzic, *Astron. J.* **132**, 2685 (2006) [arXiv:astro-ph/0509417].
- [52] D. Maurin, R. Taillet and C. Combet, arXiv:astro-ph/0609522.
- [53] T. Delahaye, F. Donato, N. Fornengo, J. Lavalle, R. Lineros, P. Salati and R. Taillet, *Astron. Astrophys.* **501**, 821 (2009) [arXiv:0809.5268 [astro-ph]].
- [54] E. A. Baltz and J. Edsjo, *Phys. Rev. D* **59**, 023511 (1999) [arXiv:astro-ph/9808243].
- [55] D. Maurin, F. Donato, R. Taillet and P. Salati, *Astrophys. J.* **555**, 585 (2001) [arXiv:astro-ph/0101231].
- [56] F. Donato, N. Fornengo, D. Maurin and P. Salati, *Phys. Rev. D* **69**, 063501 (2004) [arXiv:astro-ph/0306207].
- [57] J. D. Simon and M. Geha, *Astrophys. J.* **670**, 313 (2007) [arXiv:0706.0516 [astro-ph]].